Molecular Neurobiology

An amino acid substitution found in animals with low susceptibility to prion diseases confers a protective dominant-negative effect in prion-infected transgenic mice

--Manuscript Draft--

Manuscript Number:	MOLN-D-17-00896R1
Article Type:	Original Article
Keywords:	TSE; Prion infection; transgenic mouse models; transmissible spongiform encephalopathies; prion propagation; canine PrP
Corresponding Author:	Joaquín Castilla CIC bioGUNE SPAIN
First Author:	Alicia Otero
Order of Authors:	Alicia Otero
	Rosa Bolea
	Carlos Hedman
	Natalia Fernández-Borges
	Belén Marín
	Óscar López-Pérez
	Tomás Barrio
	Hasier Eraña
	Manuel A Sánchez-Martín
	Marta Monzón
	Juan José Badiola
	Joaquín Castilla
Abstract:	While prion diseases have been described in numerous species, some, including those of the Canidae family, appear to show resistance or reduced susceptibility. A better understanding of the factors underlying prion susceptibility is crucial for the development of effective treatment and control measures. We recently demonstrated resistance to prion infection in mice overexpressing a mutated prion protein (PrP) carrying a specific amino acid substitution characteristic of canids. Here, we show that co-expression of this mutated PrP and wild type mouse PrP in transgenic mice inoculated with different mouse-adapted prion strains (22L, ME7, RML, and 301C) significantly increases survival times (by 45% to 113%). These data indicate that this amino acid substitution confers a dominant-negative effect on PrP, attenuating the conversion of PrPC to PrPSc and delaying disease onset without altering the neuropathological properties of the prion strains. Taken together, these findings have important implications for the development of new treatment approaches for prion diseases based on dominant-negative proteins.

An amino acid substitution found in animals with low susceptibility to prion diseases confers a protective dominant-negative effect in prion-infected transgenic mice

Alicia Otero [1], Rosa Bolea [1], Carlos Hedman [1], Natalia Fernández-Borges [2], Belén Marín [1], Óscar López-Pérez [1, 3], Tomás Barrio [1], Hasier Eraña [2], Manuel A. Sánchez-Martín [4,5], Marta Monzón [1], Juan José Badiola [1], Joaquín Castilla [2, 6]*

[1] Centro de Encefalopatías y Enfermedades Transmisibles Emergentes, Facultad de Veterinaria, Universidad de Zaragoza, Zaragoza, Spain.

[2] CIC bioGUNE, Parque Tecnológico de Bizkaia, Derio, Bizkaia, Spain.

[3] Laboratorio de Genética Bioquímica (LAGENBIO), Facultad de Veterinaria, Universidad de Zaragoza, Zaragoza, Spain.

[4] Servicio de Transgénesis, Nucleus, Universidad de Salamanca, Salamanca, Spain.

[5] IBSAL, Instituto de Investigación Biomédica de Salamanca, Salamanca, Spain.

[6] IKERBASQUE, Basque Foundation for Science, Bilbao, Bizkaia, Spain.

* Corresponding author:

Joaquín Castilla

CIC bioGUNE

Parque tecnológico de Bizkaia

Derio 48160, Bizkaia, Spain

E-mail: castilla@joaquincastilla.com

Abstract

While prion diseases have been described in numerous species, some, including those of the Canidae family, appear to show resistance or reduced susceptibility. A better understanding of the factors underlying prion susceptibility is crucial for the development of effective treatment and control measures. We recently demonstrated resistance to prion infection in mice overexpressing a mutated prion protein (PrP) carrying a specific amino acid substitution characteristic of canids. Here, we show that co-expression of this mutated PrP and wild type mouse PrP in transgenic mice inoculated with different mouse-adapted prion strains (22L, ME7, RML, and 301C) significantly increases survival times (by 45% to 113%). These data indicate that this amino acid substitution confers a dominant-negative effect on PrP, attenuating the conversion of PrP^{C} to PrP^{Sc} and delaying disease onset without altering the neuropathological properties of the prion strains. Taken together, these findings have important implications for the development of new treatment approaches for prion diseases based on dominant-negative proteins.

Keywords

TSE; Prion infection; transgenic mouse models; transmissible spongiform encephalopathies; prion propagation; canine PrP

Introduction

Transmissible spongiform encephalopathies (TSEs), or prion diseases, are a group of neurodegenerative diseases of animals and humans that can be sporadic (putatively spontaneous), genetic, or acquired by infection [1]. TSEs are caused by the accumulation of a misfolded protein, the scrapie-associated prion protein (PrP^{Sc}), which is produced by posttranslational conversion of the physiologically expressed cellular prion protein (PrP^{C}) via an unknown mechanism. This abnormal form of the protein is protease resistant and is composed almost entirely of β-sheet structures [2-5]. PrP^{Sc} deposition results in spongiosis, vacuolation, neuronal death, and glial reactions in the central nervous system of affected individuals [3,6-8]

TSEs naturally affect a wide variety of mammalian species, and include Creutzfeldt–Jakob disease (CJD) in humans, scrapie in sheep and goats, bovine spongiform encephalopathy (BSE) in cattle, and chronic wasting disease (CWD) in cervids [9]. Since the emergence of BSE and its association with variant CJD (vCJD) in humans [10,11], transmission of prion diseases between species has become a major public health concern. Spongiform encephalopathies have been identified in numerous ruminant, feline, and primate species, all of which had consumed cattle meat or feed containing ruminant meat and bone meal, or were in close proximity to infected animals [12-14]. However, the absence of prion diseases in other mammals exposed to contaminated food, including rabbits, equids, and canids, suggested the existence of prion-resistant species [15]. This was further supported by unsuccessful attempts to overcome TSE transmission barriers in those species, which contributed to preserve for decades the concept of prion resistant mammals [16]. Of all putative prion-resistant species, rabbits are the most extensively studied. *In vitro* studies using protein misfolding cyclic amplification (PMCA) and subsequent *in vivo* experiments have shown that rabbits are not disease-resistant *per se*, but are poorly susceptible to prion diseases [17]. Equids represent a very interesting group of mammals that, while not completely resistant to TSEs, show a very

68 peculiar susceptibility displaying an unusual replicative phenomenon termed nonadaptative
69 prion amplification (NAPA), described in transgenic mice expressing horse PrP [18]. Moreover,
70 the use of recombinant proteins in the presence of chaotropic agents [19] and *in vitro* prion
71 amplification techniques [20] to study the propensity of prion protein misfolding in different
72 mammalian species suggest that susceptibility to prion diseases is lowest in canids. To identify
73 the specific features of canine PrP^{C} that account for its strong resistance to misfolding, we
74 previously generated a transgenic mouse model expressing a PrP variant (N158D PrP),
75 containing a single specific amino acid substitution, characteristic of the dog PrP^{C} [Fernández-
76 Borges et al. Unraveling the key to the resistance of canids to prion diseases. PLoS Pathogens
77 (second round of review)]. We found that this model was completely resistant to intracerebral
78 infection with several mouse-adapted prion strains, indicating that a single amino acid
79 substitution is sufficient to inhibit the misfolding of the mutated protein.
80 In the present study, we investigated whether this mutant could act as a dominant-
81 negative protein and prevent PrP^{Sc} formation when co-expressed with wild type (wt) PrP^{C}. To
82 this end, we created a new mouse model co-expressing wt mouse PrP^{C} and the
83 aforementioned mutant PrP variant carrying the critical dog amino acid substitution. These
84 mice were intracerebrally inoculated with different mouse-adapted prion strains and the
85 results of the *in vivo* challenge compared with those obtained in mice expressing comparable
86 levels of wt mouse prion protein. Surprisingly, co-expression of the mutated protein
87 significantly delayed the onset of disease induced by all prion strains studied. Survival periods
88 were increased by 45% to 113% with respect to mice expressing wt protein alone, thereby
89 demonstrating the dominant-negative effect of the mutant protein. Our findings show that this
90 specific dog amino acid substitution confers the protein the ability to interfere with the
91 propagation of wt prions in transgenic mice. These findings have important implications for the
92 development of therapeutic strategies against prion diseases.
93

Materials and methods

Generation and inoculation of transgenic mouse models

Three different transgenic mouse models were used in the present study: 1) Tga20 x Tga20 mice (hereafter referred to as Tga20 mice) expressing mouse PrP^C at a levels ~8-fold higher than those observed in the mouse brain [21]; Tga20 x *Prnp*$^{0/0}$ [22] (hereafter referred to as Tga20xKO mice) mice expressing mouse PrP^C at a levels ~4-fold higher than those observed in mouse brain; and 3) Tga20 x TgN158D mice [hereafter referred to as Tga20xN158D: Fernández-Borges et al. (submitted)] expressing mouse PrP^C at levels ~4-fold higher and N158D mouse PrP^C at levels ~2-fold higher than those observed in mouse brain. The murine *PRNP* promoter was used for N158D mouse PrP^C expression.

PrP expression levels from Tga20, Tga20xKO and Tga20xN158D mice were analyzed by Western blot using SAF83 (1:400) and 5C6 (1:2,000) monoclonal antibodies and compared with those obtained in TgN158DxTgN158D mice (hereafter referred to as TgN158D mice), expressing only N158D mouse PrP^C [Fernández-Borges N, et al. (submitted)]. 5C6 antibody (PRC5 antibody) was kindly provided by Dr. Glenn Telling (Prion Research Center, Colorado State University). This antibody requires asparagine at mouse PrP residue 158 [23] and therefore does not detect N158D PrP, whereas SAF83 antibody recognizes both wt and N158D mouse PrPs (Supplementary Fig. 1).

Mice aged 6 to 8 weeks were anesthetized with isoflurane and intracerebrally inoculated (left cerebral hemisphere) with mouse-adapted prion strains 22L, RML, ME7, or 301C using 20 µl of a 10% brain homogenate. Injections were administered using a 50-µl syringe and a 25-G needle. Analgesia was achieved by subcutaneous injection of buprenorphine (0.3 mg/kg). Animals were subsequently housed in filtered cages and monitored three times per week for neurologic dysfunction. Mice were euthanized by cervical

dislocation upon detection of clinical signs of terminal disease (severe ataxia, inability to stand, and poor body condition).

All experimental procedures were approved by the Ethics Committee for Animal Experiments of the University of Zaragoza (permit number: PI32/13) and performed in accordance with the recommendations for the care and use of experimental animals and in agreement with Spanish law (R.D. 1201/05).

Sample processing and histopathological evaluation

After euthanasia, brains were removed, and transversal sections from the frontal cortex and medulla oblongata were separated and frozen at -80°C for subsequent biochemical analyses. The remaining tissue was fixed in 10% formalin for neuropathological studies. After fixation, brains were cut at four standard levels for the histological evaluation of the following 9 brain regions: frontal cortex (Fc), septal area (Sa), thalamic cortex (Tc), hippocampus (Hc), thalamus (T), hypothalamus (Ht), mesencephalon (Mes), cerebellum (Cbl) and medulla oblongata (Mo) [24]. Tissues were embedded in paraffin, cut into 4-µm-thick sections on a microtome, and mounted on glass slides for staining with hematoxylin and eosin. Sections were examined using an optical microscope (Zeiss Axioskop 40), and the extent of vacuolation and spongiosis in each area was blindly evaluated and semi-quantitatively scored on a scale of 0 (absence of lesions) to 5 (high intensity lesions).

Analysis of PrP^{Sc} deposition

The intensity and distribution of PrP^{Sc} deposition was evaluated using the paraffin-embedded tissue (PET) blot method, as previously described [25]. Sections from paraffin-embedded brains (4-µm thick) were collected on a nitrocellulose membrane (0.45-µm pore size; Bio-Rad, Richmond, CA) and dried at 55°C for 24 h. After deparaffination and rehydration, sections were digested for 2 h at 56°C with 250 µg/ml proteinase-K (PK) (Applied Biosystems) in PK digestion buffer containing TBS (Tris-buffered saline) and 0.1% Brij 35P (Sigma-Aldrich). After washing with TBST (Tris buffered saline; 0.05% Tween 20), membrane-attached proteins were

denatured in 3 M guanidine thiocyanate (Sigma-Aldrich). Sections were then blocked with 1% casein in TBST and incubated with Sha31 primary monoclonal antibody (1:8000; SPI-Bio). After incubation with an alkaline phosphatase-coupled goat anti-mouse antibody (DAKO) immunostaining was visualized using NBT/BCIP (Nitro blue tetrazolium /5-bromo-4-chloro-3-indolyl-phosphate; Sigma-Aldich). PrP^{Sc} deposits were evaluated semi-quantitatively, as described for spongiform lesions, using a Zeiss Stemi DV4 stereo microscope.

Histological analysis of PrP^{C} distribution

The localization and distribution of PrP^{C} in the brains of Tga20xN158D mice was analyzed by immunohistochemistry. Brains from TgN158D mice were used as controls. Serial paraffin-embedded sections were incubated with a peroxidase blocking reagent (Dako) for 20 min followed by hydrated autoclaving at 100°C in citrate buffer for 30 min. Immunodetection was performed overnight at 4°C using SAF32 (1:1,000; SPI-Bio) and 5C6 (1:1,000) anti-PrP monoclonal antibodies. The anti-mouse Envision polymer (Dako) was used as the visualization system and DAB (diaminobenzidine, Dako) as the chromogen.

The localization of N158D PrP was analyzed using immunofluorescence and confocal imaging. Immunofluorescence staining was performed as described previously [26], with specific modifications to adapt the protocol to paraffin-embedded samples. Paraffin-embedded tissue sections from TgN158D mice were deparaffinated and rehydrated and then blocked with 1% H_2O_2 for 30 min. After pretreatment with 0,1% Triton X-100 for 3 h at room temperature, samples were subjected to hydrated autoclaving and incubated with SAF32 antibody (1:100) followed by a goat anti-mouse IgG biotin conjugate (1:100; Invitrogen) and an Alexa fluor 594 streptavidin conjugate (1:1000; Invitrogen). Sections were analyzed using a Zeiss laser-scanning confocal microscope LSM 510 (Carl Zeiss MicroImaging).

Biochemical analysis

Frozen brain sections stored for biochemical analysis, as described above, were homogenized in 1% (w/v) in PBS (phosphate buffered saline) using a ribolyzer. The resulting samples were

digested with Protease K (PK) for 1 h at 42°C, and used for Western blot. Immunodetection was performed using SAF83 ~~primary antibody~~ (SPI-Bio; 1:~~10,000~~ 400) and 5C6 (1:2,000) primary antibodies.

Data analysis

Survival times were analyzed by Kaplan-Meier survival analysis, and the resulting survival curves were compared using the log rank test (α=0.050). Differences in spongiform lesions (distribution and intensity) and PrP^{Sc} deposition profiles between different transgenic mouse models were evaluated using the non-parametric Mann-Whitney U-test, and considered significant at $p < 0.05$. GraphPad Prism version 6.0 (GraphPad Software, La Jolla, CA, USA) was used to perform all statistical analyses, generate Kaplan Meier curves, and to graph histopathology results.

Results

Co-expression of the N158D PrP substitution greatly increases survival time in inoculated mice

Three groups of mice expressing different levels of wt protein, either alone or together with N158D PrP [(Tga20 (8x), Tga20xKO (4x+0x) and Tga20xN158D (4x+2x)] (Supplementary Fig. 1) were challenged by intracerebral inoculation with the 22L, RML, 301C, or ME7 mouse-adapted prion strains. Owing to its high levels of PrP^{C} expression in the brain (~8 fold higher than wt mice), the TSE incubation period in the Tga20 mouse is relatively short, making it a useful model for prion research. Moreover, the histopathological and biochemical features of several mouse-adapted TSE strains, including those used in the present study, are well defined in this transgenic model [21,27]. Tga20xN158D mice were used to achieve co-expression of the wt and N158D PrP. Tga20xKO mice were selected as controls, given that their wt PrP^{C} expression level is identical to that of Tga20xN158D mice. No significant differences were observed in electrophoretic migration patterns between the different mouse lines (Supplementary Fig. 1).

196 In addition, both wt and N158D PrPs are present in high amounts, and are distributed normally
197 in the brain of transgenic mice (Supplementary Fig. 2).

198 Tga20xN158D mice inoculated with the 22L, RML, 301C, or ME7 prion strains showed
199 increases in survival times of 113%, 45%, 71%, and 49%, respectively, as compared with
200 Tga20xKO mice, which express the same amount of wt PrP^C (Table 1). Significant differences
201 were observed between genotypes for all inocula (Fig. 1). In the case of the 301C strain,
202 survival times in Tga20xN158D mice were not as homogeneous as those observed for the
203 other strains, as evidenced by less steep decline in the Kaplan-Meier curve (Fig. 1).

204 Although survival time was significantly increased in Tga20xN158D mice, the clinical
205 presentation in these mice was indistinguishable from that of mice expressing only the wt
206 protein. Mice developed clinical signs typical of TSEs in rodents, including poor hair coat
207 condition and kyphosis in the early stages of the disease, followed by proprioceptive deficits,
208 head twitching, and progressive ataxia, which became severe in terminal stages. However,
209 certain clinical signs were more evident in animals infected with a given inoculum (e.g., the
210 opisthotonos observed in all three genotypes of mice inoculated with the 22L strain, a sign that
211 may be due to cerebellar lesions).

212 Expression of the dominant-negative protein did not alter the neuropathological features of
213 the disease

214 Despite the substantial prolongation of survival time in mice co-expressing the N158D PrP
215 substitution, an exhaustive comparison of the two models expressing equivalent levels of wt
216 PrP^C (Tga20xKO and Tga20xN158D mice) revealed no significant differences in terms of the
217 neuropathological characteristics of the disease. Lesion profiles and prion protein deposition
218 patterns, evaluated semi-quantitatively on a scale of 0 to 5, were very similar between
219 different genotypes inoculated with the same strain (Figs. 2 and 3). Our results are consistent
220 with those of another study in which Tga20 mice were infected with all the same inocula [27],
221 indicating that the mouse-adapted strains used in the present study retained their

222 characteristic histopathological features and PrP^{Sc} deposition profiles. All mice infected with
223 the 22L strain developed particularly severe spongiform lesions and showed marked PrP^{Sc}
224 deposition in the T, Ht, Mes and Mo (Figs. 2 and 3a). Inoculation with the RML strain resulted
225 in intense histopathological changes and PrP^{Sc} deposition predominantly in the T, Mes, and Mo
226 (Figs. 2 and 3a), with low vacuolation scores observed in the Cbl. The spongiform lesions
227 caused by the 301C strain were mainly located in the T, Mes, and Mo (Fig. 2). Compared with
228 the other strains used, this mouse-adapted BSE strain produced slightly less intense PrP^{Sc}
229 deposition throughout the brain (Fig. 3a), as described previously in wt mice [28]. Finally,
230 inoculation with ME7 resulted in severe spongiosis and vacuolation in the Sa, T, Ht, and
231 brainstem (Fig. 2) and very intense PrP^{Sc} deposition in the Hc, T, and Sa in all genotypes, (Fig.
232 3a), indicating that the main features of the ME7 strain, as previously described in Tga20 mice
233 [27], were preserved (Fig. 3b).

234 The results of biochemical analyses were consistent with the histopathological
235 findings. No significant differences in PrP glycosylation and electrophoretic mobility patterns
236 between Tga20, Tga20xKO, and Tga20xN158D mice were observed for any of the strains
237 inoculated (Fig. 4). We further investigated whether the similarities observed between
238 Tga20xKO and Tga20xN158D mice regarding the histopathological and biochemical features of
239 the disease could be related to an exclusive conversion of wt PrP^{C}. Serial dilutions of brain
240 homogenates from 22L infected Tga20xKO and Tga20xN158D mice were analyzed for PrP^{res}
241 using two different antibodies: 5C6, which is unable to detect N158D PrP since it requires the
242 presence of asparagine at codon 158 [23], and SAF83, which detects both wt and N158D PrPs.
243 No differences were observed in the amount of PrP^{res} detected by these antibodies in
244 Tga20xN158D mice, indicating that only wt PrP^{C} was converted (Supplementary Fig. 3).
245

246 Discussion

247 Certain PrP polymorphisms are strongly linked to susceptibility/resistance to prion diseases.
248 This relationship has been well documented in sheep, leading to the establishment of five
249 haplotypic PrP gene variants associated with scrapie susceptibility [29]. Among the three main
250 polymorphisms of ovine *PRNP*, variations at codon 171 appear to be the principal
251 determinants of resistance to classical scrapie; sheep with arginine at this specific residue are
252 resistant to natural [30] and experimental [31,32] scrapie infection. Heterozygosity at certain
253 PrP positions also exerts protective effects against human prion diseases [33].
254 The ability of certain variant proteins to interfere with co-expressed wt PrP and block
255 prion replication is known as a dominant-negative effect. This has been experimentally
256 reproduced in cells and in transgenic mice, and may have implications for the development of
257 therapeutic strategies for prion diseases [34-37]. The use of PMCA in *in vitro* studies has
258 proved an efficient means of testing a wide variety of PrPs with different substitutions in order
259 to identify the most appropriate dominant-negative changes [16].
260 In the search for PrPs that exert a consistent and potent inhibitory effect on *in vivo*
261 prion propagation, it seems reasonable to begin with PrPs from species with demonstrated low
262 susceptibility to prion diseases. For the purposes of this study, we selected dog prion protein,
263 in which low susceptibility has been proven [19,20]. Using cell and brain-based PMCA, we
264 previously demonstrated that the substitution of asparagine with aspartic or glutamic acid at
265 codon 163, a distinctive substitution from the Canidae family [38], strongly inhibits prion
266 replication *in vitro*. Moreover, we found that when transgenic mice overexpressing a PrP
267 variant carrying this substitution were challenged with several mouse-adapted prion strains,
268 they were completely resistant to prion infection [Fernández-Borges N, et al. (submitted)].
269 Based on these findings, we investigated whether the co-expression of this mutant PrP
270 together with wt mouse PrP could interfere with prion propagation, thereby preventing or
271 delaying the onset of the disease *in vivo*.

Co-expression of both proteins dramatically increased survival times after inoculation with any of the four mouse-adapted prion strains tested (22L, RML, 301C and ME7). Furthermore, survival times in Tga20 and Tga20xKO mice differed significantly. This was not unexpected since PrP^{C} expression levels dramatically influence the incubation time in prion diseases, and expression levels of PrP^{C} are inversely proportional to the duration of the survival period [39,40]. However, it is important to note that, in our study, the appropriate comparison of survival period is with that of mice expressing an equivalent amount of wt PrP (i.e., Tga20xKO vs. Tga20xN158D mice; Table 1).

The elongation of the survival times produced by the co-expression of an exogenous protein can be the result of several processes. We observed that, when PrP^{res} levels from Tga20xKO and Tga20xN158D mice culled at different days post inoculation (dpi) were compared, Tga20xKO mice showed higher amounts of PrP^{res}, even at shorter incubation periods than Tga20xN158D mice (Supplementary Fig. 4). Thus, we can suggest that the longer survival times observed in Tga20xN158D mice may be due to a slower rate of misfolding of the wt PrP, therefore producing a delayed accumulation of PrP^{Sc}. However, the molecular mechanisms by which N158D PrP delays prion propagation remain unclear. Several theories, most of them developed using scrapie infected cell models, have been proposed to explain how dominant-negative proteins inhibit prion propagation. Although differing only at one position from the wt PrP, dominant-negative proteins could obstruct the interactions between similar PrP monomers [39,41-43] since the difference between mutant and wt PrP could make them structurally incompatible [44]. This dissimilarity could interfere with the rate of formation [37] and the stability of PrP^{Sc} polymers [41,45]. In addition, it has been also proposed that dominant-negative proteins may compete with wt PrP^{C} for binding to newly formed PrP^{Sc} molecules [45,46]. Thus, the prolongation in survival times observed in the present study might also be the result of a greater affinity of N158D PrP for interacting with PrP^{Sc} than that of wt PrP. Due to the apparent resistance of N158D PrP to misfold

298 (Supplementary Fig. 3), a competition of this mutant and wt PrP for the same binding site in
299 PrP^{Sc} would explain the delay of the disease observed in Tga20xN158D mice, as previously
300 reported [45,46].

301 Although survival times were significantly increased in Tga20xN158D mice inoculated
302 with all experimental strains, this effect was not homogeneous for all strains. The greatest
303 increase was observed in mice inoculated with the 22L strain: survival time in mice carrying the
304 N158D PrP variant was 113% longer than that of controls. The smallest increase in survival
305 times was observed in RML-inoculated Tga20xN158D mice (45% increase). It is well
306 demonstrated that when propagated *in vivo,* distinct mouse-adapted prion strains differ in
307 terms of incubation period, as well as their biochemical and neuropathological features [47-
308 50]. Strains can also show biophysical, molecular, and, as in the case of the strains used in the
309 present study, ultrastructural differences [51,52]. These findings could explain that different
310 tertiary and/or quaternary structures were also differentially affected by the blockade of a
311 dominant-negative protein. ~~The molecular mechanisms by which N158D PrP partially blocks~~
312 ~~prion propagation remain unclear.~~ Our findings suggest that the dominant-negative effect of
313 this mutant protein is stronger with certain strains (22L and 301C) than with others (RML and
314 ME7). Other dominant-negative proteins have been also reported to interfere with the
315 generation of PrP^{Sc} in a strain-specific manner. As an example, Q218K PrP strongly inhibits the
316 misfolding of co-expressed wt PrP in Chandler-infected cells but produces a much weaker
317 inhibition with 22L strain. This distinct effect was attributed to the structural differences,
318 determined by IR spectroscopy, between Chandler and 22L strains [53]. As aforementioned,
319 we cannot know for certain what precise molecular mechanisms are involved in the partial
320 dominance exerted by N158D PrP. However, if the dominant-negative protein blocks fibril
321 growth, ultrastructural differences between strains could account for the differential effect
322 (45%–113% increase) of the dominant-negative protein on the survival period.

The dominant-negative effect of certain mutant PrPs on PrP^{Sc} formation has been already demonstrated *in vivo* in transgenic mice co-expressing wt PrP [36]. In that study, mice expressing PrPs containing ovine and human TSE resistance-associated substitutions were not completely resistant to prion formation when mutant and wt mouse PrPs were co-expressed. Our findings are in agreement with those results, and demonstrate that minimal amino acid changes can produce highly efficient dominant-negative variants able to double the survival period when co-expressed with wt mouse PrP^{C}. Extrapolating these findings to humans, in which the incubation period of prion diseases can last for decades, it seems possible that affected individuals may never develop clinical signs. The ability shown by certain PrP molecules with single residue substitutions to interfere with the misfolding of the endogenous PrP^{C} has already been demonstrated. However, most of the approaches have been performed using cell cultures [34,41,53], whereas *in vivo* studies are limited [36,54]. In addition, the dominant-negative effects described for this type of molecules, albeit potent, have been demonstrated against a limited number of strains [36,41,53]. Herein, we show that N158D PrP produces a dominant-negative inhibition in the propagation of a variety of prion strains, of both scrapie (22L, RML and ME7) and BSE (301C) origins. The delay of the disease was not homogeneous among the strains despite showing inhibition against the propagation of all of them. When describing dominant-negative PrPs it is important to check their ability to interfere with the propagation of prions from different origins and characteristics. Other naturally occurring amino acid variants of PrP^{C}, such as sheep Q171R, have demonstrated a strong dominant-negative inhibition in the propagation of scrapie strains [34-36,45]. However, it has been shown that sheep with Q171R are susceptible to atypical scrapie [55] as well as BSE [56]. Thus, our study suggests that N158D PrP, a substitution found in canids in which no natural prion diseases have been reported, may be a dominant-negative protein with a broader inhibitory effect.

348 The prolongation of the incubation period seen in the present study was less dramatic than
349 that reported by Perrier and coworkers in RML-inoculated mice co-expressing equal amounts
350 of wt PrP and dominant-negative PrP. However, wt PrP expression levels in our Tga20xN158D
351 mice are 4 times higher than those of wt mice, making it more difficult to fully block prion
352 formation. It cannot be ruled out that if an equimolecular amount of dominant-negative PrP
353 and wt PrP is required for the complete blockade of prion propagation, we would need to
354 double the amount of N158D PrP. The dose dependent, dominant-negative inhibition by other
355 similar molecules has already been demonstrated [41,45,36], showing that certain dominant-
356 negative proteins need to be present in high amounts to inhibit endogenous PrP^{C} conversion
357 [45,36]. We have observed that N158D PrP, even being expressed at lower levels than wt PrP,
358 is able to significantly extend the survival period in Tga20xN158D mice.
359 The neuropathological changes seen in our Tga20xN158D mice were very similar to
360 those observed in mice expressing only wt PrP, with few significant differences observed in
361 terms of lesion and PrP^{Sc} deposition profiles (Figs. 2 and 3). These findings, coupled with the
362 complete resistance to intracerebral challenge seen in mice expressing N158D mutant protein
363 only [Fernández-Borges et al (submitted)], could lead us to think that the pathological form
364 detected and therefore the neuropathological hallmarks observed in Tga20xN158D mice are
365 due only to the conversion of the mouse wt protein. Fortunately, the expression of aspartic
366 acid at 158 residue of mouse N158D PrP^{C} impedes the epitope recognition of 5C6 antibody
367 [23], and therefore it allows discrimination between wt and N158D PrP^{C}. Our results indicate
368 that only mouse wt PrP^{C} was converted in Tga20xN158D mice (Supplementary Fig. 3).
369 ~~However, in our Tga20xN158D model, in which wt and mutant PrP are co-expressed, we~~
370 ~~cannot rule out the possibility that misfolding of the mutated PrP may occur, albeit to a lesser~~
371 ~~extent. Unfortunately, given that the two forms differ by a single amino acid, we cannot~~
372 ~~establish whether this occurs.~~ ~~Nonetheless, we found that~~ Accordingly with this suggestion,
373 most of the pathological features previously described in Tga20 mice inoculated with the

strains used in the present study [27] were reproduced in Tga20xN158D mice. All of the prion strains tested produced marked spongiosis and PrP^{Sc} deposition in both the thalamus and brainstem of Tga20xN158D mice (Figs. 2 and 3), regions previously proposed as clinical target areas of these strains in Tga20 mice [27]. In mice co-expressing N158D PrP, these different prion strains retained their specific pathological characteristics, as evidenced by the marked PrP^{Sc} deposition in the hippocampus of ME7-inoculated mice (Fig. 3b) [27] and the characteristic affectation of the cerebellum in those inoculated with the 22L strain [57]. Expression of the dominant-negative protein therefore appears not to have affected the characteristic pathological hallmarks of these strains, indicating that the increase in survival times observed in Tga20xN158D mice is not due to strain modifications caused by the amino acid substitution of the dominant-negative protein.

Based on our findings, we conclude that N158D PrP acts as a dominant-negative protein to partially block the conversion of PrP^{C} to PrP^{Sc}, and is thus a promising candidate for gene therapy strategies for the treatment of TSEs.

Acknowledgments

This work was supported financially by grants from the Spanish (AGL2015-65046-C2-1-R, AGL2015-65560-R, and PCIN-2013-065) and Basque (2014111157) governments. We thank MINECO for the Severo Ochoa Excellence Accreditation (SEV-2016-0644). The authors would like to thank the following for their support: the IKERBasque Foundation, the staff at the CIC bioGUNE animal facility, Dr. Belén Pintado for the Tga20 mouse embryo rederivation, Dr. Glenn Telling for kindly providing the 5C6 antibody and Patricia Piñeiro, Silvia Ruiz and Sonia Gómez ~~from the Centro de Encefalopatías y Enfermedades Transmisibles Emergentes~~ for their technical assistance. The authors would also like to acknowledge Sara Gutiérrez for the image editing. Alicia Otero was supported by a research grant from the Government of Aragón (C020/2014) co-financed by the European Social Fund.

Compliance with ethical standards

This study was approved by the Ethics Committee for Animal Experiments of the University of Zaragoza (permit number PI32/13) and was performed in accordance with the recommendations for the care and use of experimental animals and with Spanish national law (R.D. 1201/05).

Conflict of interest

The authors declare that they have no conflict of interest.

References

1. Prusiner SB (1998) The prion diseases. Brain Pathol 8 (3):499-513

2. Prusiner SB (1998) Prions. Proc Natl Acad Sci U S A 95 (23):13363-13383

3. Prusiner SB (1982) Novel proteinaceous infectious particles cause scrapie. Science 216 (4542):136-144

4. Smirnovas V, Baron GS, Offerdahl DK, Raymond GJ, Caughey B, Surewicz WK (2011) Structural organization of brain-derived mammalian prions examined by hydrogen-deuterium exchange. Nat Struct Mol Biol 18 (4):504-506. doi:10.1038/nsmb.2035

5. Vazquez-Fernandez E, Vos MR, Afanasyev P, Cebey L, Sevillano AM, Vidal E, Rosa I, Renault L, Ramos A, Peters PJ, Fernandez JJ, van Heel M, Young HS, Requena JR, Wille H (2016) The Structural Architecture of an Infectious Mammalian Prion Using Electron Cryomicroscopy. PLoS Pathog 12 (9):e1005835. doi:10.1371/journal.ppat.1005835

6. Fraser H (1976) The pathology of a natural and experimental scrapie. Front Biol 44:267-305

7. Budka H, Aguzzi A, Brown P, Brucher JM, Bugiani O, Gullotta F, Haltia M, Hauw JJ, Ironside JW, Jellinger K, et al. (1995) Neuropathological diagnostic criteria for Creutzfeldt-Jakob disease (CJD) and other human spongiform encephalopathies (prion diseases). Brain Pathol 5 (4):459-466

8. Vidal E, Acin C, Foradada L, Monzon M, Marquez M, Monleon E, Pumarola M, Badiola JJ, Bolea R (2009) Immunohistochemical characterisation of classical scrapie neuropathology in sheep. J Comp Pathol 141 (2-3):135-146. doi:10.1016/j.jcpa.2009.04.002

9. Collins SJ, Lawson VA, Masters CL (2004) Transmissible spongiform encephalopathies. Lancet 363 (9402):51-61. doi:10.1016/S0140-6736(03)15171-9

10. Will RG, Ironside JW, Zeidler M, Cousens SN, Estibeiro K, Alperovitch A, Poser S, Pocchiari M, Hofman A, Smith PG (1996) A new variant of Creutzfeldt-Jakob disease in the UK. Lancet 347 (9006):921-925

434 11. Bruce ME, Will RG, Ironside JW, McConnell I, Drummond D, Suttie A, McCardle L, Chree A,
435 Hope J, Birkett C, Cousens S, Fraser H, Bostock CJ (1997) Transmissions to mice indicate that
436 'new variant' CJD is caused by the BSE agent. Nature 389 (6650):498-501. doi:10.1038/39057
437 12. Kirkwood JK, Cunningham AA (1994) Epidemiological observations on spongiform
438 encephalopathies in captive wild animals in the British Isles. Vet Rec 135 (13):296-303
439 13. Kirkwood JK, Cunningham AA, Wells GA, Wilesmith JW, Barnett JE (1993) Spongiform
440 encephalopathy in a herd of greater kudu (Tragelaphus strepsiceros): epidemiological
441 observations. Vet Rec 133 (15):360-364
442 14. Sigurdson CJ, Miller MW (2003) Other animal prion diseases. Br Med Bull 66:199-212
443 15. Fernandez-Borges N, Chianini F, Eraña H, Vidal E, Eaton SL, Pintado B, Finlayson J, Dagleish
444 MP, Castilla J (2012) Naturally prion resistant mammals: a utopia? Prion 6 (5):425-429.
445 doi:10.4161/pri.22057
446 16. Fernandez-Borges N, de Castro J, Castilla J (2009) In vitro studies of the transmission
447 barrier. Prion 3 (4):220-223
448 17. Chianini F, Fernandez-Borges N, Vidal E, Gibbard L, Pintado B, de Castro J, Priola SA,
449 Hamilton S, Eaton SL, Finlayson J, Pang Y, Steele P, Reid HW, Dagleish MP, Castilla J (2012)
450 Rabbits are not resistant to prion infection. Proc Natl Acad Sci U S A 109 (13):5080-5085.
451 doi:10.1073/pnas.1120076109
452 18. Bian J, Khaychuk V, Angers RC, Fernandez-Borges N, Vidal E, Meyerett-Reid C, Kim S, Calvi
453 CL, Bartz JC, Hoover EA, Agrimi U, Richt JA, Castilla J, Telling GC (2017) Prion replication
454 without host adaptation during interspecies transmissions. Proc Natl Acad Sci U S A 114
455 (5):1141-1146. doi:10.1073/pnas.1611891114
456 19. Khan MQ, Sweeting B, Mulligan VK, Arslan PE, Cashman NR, Pai EF, Chakrabartty A (2010)
457 Prion disease susceptibility is affected by beta-structure folding propensity and local side-chain
458 interactions in PrP. Proc Natl Acad Sci U S A 107 (46):19808-19813.
459 doi:10.1073/pnas.1005267107

460 20. Vidal E, Fernandez-Borges N, Pintado B, Ordoñez M, Marquez M, Fondevila D, Torres JM,
461 Pumarola M, Castilla J (2013) Bovine spongiform encephalopathy induces misfolding of alleged
462 prion-resistant species cellular prion protein without altering its pathobiological features. J
463 Neurosci 33 (18):7778-7786. doi:10.1523/JNEUROSCI.0244-13.2013
464 21. Fischer M, Rulicke T, Raeber A, Sailer A, Moser M, Oesch B, Brandner S, Aguzzi A,
465 Weissmann C (1996) Prion protein (PrP) with amino-proximal deletions restoring susceptibility
466 of PrP knockout mice to scrapie. EMBO J 15 (6):1255-1264
467 22. Manson JC, Clarke AR, Hooper ML, Aitchison L, McConnell I, Hope J (1994) 129/Ola mice
468 carrying a null mutation in PrP that abolishes mRNA production are developmentally normal.
469 Mol Neurobiol 8 (2-3):121-127. doi:10.1007/BF02780662
470 23. Kang HE, Weng CC, Saijo E, Saylor V, Bian J, Kim S, Ramos L, Angers R, Langenfeld K,
471 Khaychuk V, Calvi C, Bartz J, Hunter N, Telling GC (2012) Characterization of conformation-
472 dependent prion protein epitopes. J Biol Chem 287 (44):37219-37232.
473 doi:10.1074/jbc.M112.395921
474 24. Fraser H, Dickinson AG (1968) The sequential development of the brain lesion of scrapie in
475 three strains of mice. J Comp Pathol 78 (3):301-311
476 25. Schulz-Schaeffer WJ, Tschoke S, Kranefuss N, Drose W, Hause-Reitner D, Giese A, Groschup
477 MH, Kretzschmar HA (2000) The paraffin-embedded tissue blot detects PrP(Sc) early in the
478 incubation time in prion diseases. Am J Pathol 156 (1):51-56. doi:10.1016/S0002-
479 9440(10)64705-0
480 26. Sarasa R, Martinez A, Monleon E, Bolea R, Vargas A, Badiola JJ, Monzon M (2012)
481 Involvement of astrocytes in transmissible spongiform encephalopathies: a confocal
482 microscopy study. Cell Tissue Res 350 (1):127-134. doi:10.1007/s00441-012-1461-1
483 27. Karapetyan YE, Saa P, Mahal SP, Sferrazza GF, Sherman A, Sales N, Weissmann C, Lasmezas
484 CI (2009) Prion strain discrimination based on rapid in vivo amplification and analysis by the
485 cell panel assay. PLoS One 4 (5):e5730. doi:10.1371/journal.pone.0005730

28. Tuzi NL, Cancellotti E, Baybutt H, Blackford L, Bradford B, Plinston C, Coghill A, Hart P, Piccardo P, Barron RM, Manson JC (2008) Host PrP glycosylation: a major factor determining the outcome of prion infection. PLoS Biol 6 (4):e100. doi:10.1371/journal.pbio.0060100

29. Belt PB, Muileman IH, Schreuder BE, Bos-de Ruijter J, Gielkens AL, Smits MA (1995) Identification of five allelic variants of the sheep PrP gene and their association with natural scrapie. J Gen Virol 76 (Pt 3):509-517. doi:10.1099/0022-1317-76-3-509

30. Westaway D, Zuliani V, Cooper CM, Da Costa M, Neuman S, Jenny AL, Detwiler L, Prusiner SB (1994) Homozygosity for prion protein alleles encoding glutamine-171 renders sheep susceptible to natural scrapie. Genes Dev 8 (8):959-969

31. Clouscard C, Beaudry P, Elsen JM, Milan D, Dussaucy M, Bounneau C, Schelcher F, Chatelain J, Launay JM, Laplanche JL (1995) Different allelic effects of the codons 136 and 171 of the prion protein gene in sheep with natural scrapie. J Gen Virol 76 (Pt 8):2097-2101. doi:10.1099/0022-1317-76-8-2097

32. Hunter N, Cairns D, Foster JD, Smith G, Goldmann W, Donnelly K (1997) Is scrapie solely a genetic disease? Nature 386 (6621):137. doi:10.1038/386137a0

33. Shibuya S, Higuchi J, Shin RW, Tateishi J, Kitamoto T (1998) Codon 219 Lys allele of PRNP is not found in sporadic Creutzfeldt-Jakob disease. Ann Neurol 43 (6):826-828. doi:10.1002/ana.410430618

34. Kaneko K, Zulianello L, Scott M, Cooper CM, Wallace AC, James TL, Cohen FE, Prusiner SB (1997) Evidence for protein X binding to a discontinuous epitope on the cellular prion protein during scrapie prion propagation. Proc Natl Acad Sci U S A 94 (19):10069-10074

35. Zulianello L, Kaneko K, Scott M, Erpel S, Han D, Cohen FE, Prusiner SB (2000) Dominant-negative inhibition of prion formation diminished by deletion mutagenesis of the prion protein. J Virol 74 (9):4351-4360

510 36. Perrier V, Kaneko K, Safar J, Vergara J, Tremblay P, DeArmond SJ, Cohen FE, Prusiner SB,
511 Wallace AC (2002) Dominant-negative inhibition of prion replication in transgenic mice. Proc
512 Natl Acad Sci U S A 99 (20):13079-13084. doi:10.1073/pnas.182425299
513 37. Lee CI, Yang Q, Perrier V, Baskakov IV (2007) The dominant-negative effect of the Q218K
514 variant of the prion protein does not require protein X. Protein Sci 16 (10):2166-2173.
515 doi:10.1110/ps.072954607
516 38. Stewart P, Campbell L, Skogtvedt S, Griffin KA, Arnemo JM, Tryland M, Girling S, Miller MW,
517 Tranulis MA, Goldmann W (2012) Genetic predictions of prion disease susceptibility in
518 carnivore species based on variability of the prion gene coding region. PLoS One 7 (12):e50623.
519 doi:10.1371/journal.pone.0050623
520 39. Prusiner SB, Scott M, Foster D, Pan KM, Groth D, Mirenda C, Torchia M, Yang SL, Serban D,
521 Carlson GA, et al. (1990) Transgenetic studies implicate interactions between homologous PrP
522 isoforms in scrapie prion replication. Cell 63 (4):673-686
523 40. Bueler H, Raeber A, Sailer A, Fischer M, Aguzzi A, Weissmann C (1994) High prion and PrPSc
524 levels but delayed onset of disease in scrapie-inoculated mice heterozygous for a disrupted PrP
525 gene. Mol Med 1 (1):19-30
526 41. Priola SA, Caughey B, Race RE, Chesebro B (1994) Heterologous PrP molecules interfere
527 with accumulation of protease-resistant PrP in scrapie-infected murine neuroblastoma cells. J
528 Virol 68 (8):4873-4878
529 42. Bolton DC, Bendheim PE (1988) A modified host protein model of scrapie. Ciba Found Symp
530 135:164-181
531 43. Hope J, Morton LJ, Farquhar CF, Multhaup G, Beyreuther K, Kimberlin RH (1986) The major
532 polypeptide of scrapie-associated fibrils (SAF) has the same size, charge distribution and N-
533 terminal protein sequence as predicted for the normal brain protein (PrP). EMBO J 5 (10):2591-
534 2597

535 44. Jahandideh S, Jamalan M, Faridounnia M (2015) Molecular dynamics study of the
536 dominant-negative E219K polymorphism in human prion protein. J Biomol Struct Dyn 33
537 (6):1315-1325. doi:10.1080/07391102.2014.945486
538 45. Geoghegan JC, Miller MB, Kwak AH, Harris BT, Supattapone S (2009) Trans-dominant
539 inhibition of prion propagation in vitro is not mediated by an accessory cofactor. PLoS Pathog 5
540 (7):e1000535. doi:10.1371/journal.ppat.1000535
541 46. Yuan J, Zhan YA, Abskharon R, Xiao X, Martinez MC, Zhou X, Kneale G, Mikol J, Lehmann S,
542 Surewicz WK, Castilla J, Steyaert J, Zhang S, Kong Q, Petersen RB, Wohlkonig A, Zou WQ (2013)
543 Recombinant human prion protein inhibits prion propagation in vitro. Sci Rep 3:2911.
544 doi:10.1038/srep02911
545 47. Fraser H, Dickinson AG (1973) Scrapie in mice. Agent-strain differences in the distribution
546 and intensity of grey matter vacuolation. J Comp Pathol 83 (1):29-40
547 48. Bruce ME, McConnell I, Fraser H, Dickinson AG (1991) The disease characteristics of
548 different strains of scrapie in Sinc congenic mouse lines: implications for the nature of the
549 agent and host control of pathogenesis. J Gen Virol 72 (Pt 3):595-603. doi:10.1099/0022-1317-
550 72-3-595
551 49. Bruce ME (1993) Scrapie strain variation and mutation. Br Med Bull 49 (4):822-838
552 50. Baron T, Crozet C, Biacabe AG, Philippe S, Verchere J, Bencsik A, Madec JY, Calavas D,
553 Samarut J (2004) Molecular analysis of the protease-resistant prion protein in scrapie and
554 bovine spongiform encephalopathy transmitted to ovine transgenic and wild-type mice. J Virol
555 78 (12):6243-6251. doi:10.1128/JVI.78.12.6243-6251.2004
556 51. Kascsak RJ, Rubenstein R, Merz PA, Carp RI, Wisniewski HM, Diringer H (1985) Biochemical
557 differences among scrapie-associated fibrils support the biological diversity of scrapie agents. J
558 Gen Virol 66 (Pt 8):1715-1722. doi:10.1099/0022-1317-66-8-1715

559 52. Sim VL, Caughey B (2009) Ultrastructures and strain comparison of under-glycosylated
560 scrapie prion fibrils. Neurobiol Aging 30 (12):2031-2042.
561 doi:10.1016/j.neurobiolaging.2008.02.016
562 53. Atarashi R, Sim VL, Nishida N, Caughey B, Katamine S (2006) Prion strain-dependent
563 differences in conversion of mutant prion proteins in cell culture. J Virol 80 (16):7854-7862.
564 doi:10.1128/JVI.00424-06
565 54. Telling GC, Scott M, Mastrianni J, Gabizon R, Torchia M, Cohen FE, DeArmond SJ, Prusiner
566 SB (1995) Prion propagation in mice expressing human and chimeric PrP transgenes implicates
567 the interaction of cellular PrP with another protein. Cell 83 (1):79-90
568 55. Buschmann A, Biacabe AG, Ziegler U, Bencsik A, Madec JY, Erhardt G, Luhken G, Baron T,
569 Groschup MH (2004) Atypical scrapie cases in Germany and France are identified by discrepant
570 reaction patterns in BSE rapid tests. J Virol Methods 117 (1):27-36.
571 doi:10.1016/j.jviromet.2003.11.017
572 56. Houston F, Goldmann W, Chong A, Jeffrey M, Gonzalez L, Foster J, Parnham D, Hunter N
573 (2003) Prion diseases: BSE in sheep bred for resistance to infection. Nature 423 (6939):498.
574 doi:10.1038/423498a
575 57. Fraser H (1979) Neuropathology of scrapie: the precision of the lesions and their diversity.
576 In: Prusiner SB, Hadlow WJ (eds) Slow transmissible diseases of the nervous system, vol 1.
577 Academic Press New York, pp 387-406

578

Table 1. Inoculation of Tga20, Tga20xKO, and Tga20xN158D mice with mouse-adapted prion strains.

Inoculum	Model	PrP expression levels		Attack rate[a]	Survival time (dpi) (mean±SEM)[b]	Relative increase in survival time (%)[c]
		wt	Mutant (N158D)			
22L	Tga20xTga20	8x	0x	6/6 (100%)	91±2	-
	Tga20xKO	4x	0x	6/6 (100%)	98±2	-
	Tga20xN158D	4x	2x	11[d]/11 (100%)	209±3	113%
RML	Tga20xTga20	8x	0x	6/6 (100%)	70±3	-
	Tga20xKO	4x	0x	6/6 (100%)	88±1	-
	Tga20xN158D	4x	2x	11[d]/11 (100%)	128±3	45%
301C	Tga20xTga20	8x	0x	6/6 (100%)	75±1	-
	Tga20xKO	4x	0x	6/6 (100%)	92±4	-
	Tga20xN158D	4x	2x	12/12 (100%)	157±17	71%
ME7	Tga20xTga20	8x	0x	6/6 (100%)	96±2	-
	Tga20xKO	4x	0x	6/6 (100%)	101±2	-
	Tga20xN158D	4x	2x	10[d] /10 (100%)	150±3	49%

[a] Data based on PrP^{res} detection.

[b] Survival times were calculated as the number of days between inoculation and euthanasia, provided that the mouse developed clinical signs consistent with a TSE. Survival times are expressed as mean (± SEM) number of dpi.

SEM, standard error of the mean; dpi, days post-inoculation.

[c] Extension of the survival times in Tga20xN158D mice inoculated with each strain was calculated as the difference between the average survival time of Tga20xN158D and that of Tga20xKO expressed in relative percentages to the average survival times of Tga20xKO.

[d] Animals from the 22L (1), RML (1), and ME7 (2) inoculation groups died due to concomitant diseases during the initial stages of the study and were excluded from the analyses. These animals exhibited no spongiform lesions or PrP^{Sc} deposits and were not included in calculations of the SEM or attack rate.

Legends of figures

Fig. 1 Survival curves for Tga20, Tga20xKO, and Tga20xN158D mice challenged with different mouse-adapted prion strains. Comparison of Tga20xN158D curves with Tga20xKO curves using the log rank test (α=0.050) revealed very significant differences for the 22L, RML, and ME7 ($p<0.0001$) and the 301C ($p<0.0033$) inoculation groups. Survival curves for Tga20 mice inoculated with the corresponding strains are also shown. Tga20xN158D mice infected with the 22L, RML, 301C, or ME7 prion strains showed relative increases in survival times of 113%, 45%, 71%, and 49%, respectively when compared with those of Tga20xKO mice.

Fig. 2 Brain lesion profiles of Tga20, Tga20xKO, and Tga20xN158D mice inoculated with different mouse-adapted prion strains. Spongiosis and vacuolation were evaluated semiquantitatively on a scale of 0 (absence of lesions) to 5 (high intensity lesions) in the following 9 brain areas: frontal cortex (Fc), septal area (Sa), thalamic cortex (Tc), hippocampus (Hc), thalamus (T), hypothalamus (Ht), mesencephalon (Mes), cerebellum (Cbl) and medulla oblongata (Mo). Comparison of the lesion profiles of Tga20xKO and Tga20xN158D mice revealed a very similar lesion distribution (*$p<0.05$, Mann-Whitney U-test).

Fig. 3 (a) PrP^{Sc} deposition profiles in the brains of Tga20, Tga20xKO, and Tga20xN158D mice inoculated with 22L, RML, 301C, or ME7 prion strains. PrP^{Sc} deposition was evaluated semiquantitatively on a scale of 0 (absence of deposits) to 5 (high intensity deposition) in the following 9 brain areas: frontal cortex (Fc), septal area (Sa), thalamic cortex (Tc), hippocampus (Hc), thalamus (T), hypothalamus (Ht), mesencephalon (Mes), cerebellum (Cbl) and medulla oblongata (Mo). Comparison of the PrP^{Sc} deposition profiles of Tga20xKO and Tga20xN158D mice revealed almost identical PrP^{Sc} profiles (*$p<0.05$, Mann-Whitney U-test). **(b)** PET blot images of coronal sections of the mesencephalon from Tga20xKO and Tga20xN158D mice

615 inoculated with the RML or ME7 strain. Note that the PrP^{Sc} deposition profile of mice
616 expressing the mutant PrP is almost identical to that of Tga20xKO mice. Moreover, the
617 characteristic deposition patterns of the inoculated strains are retained: note the marked
618 deposition in the hippocampus in ME7-inoculated mice (arrows), a feature not observed in
619 RML-inoculated mice.

620

621 **Fig. 4** PrP^{res} detection from 22L, ME7, 301C and RML inoculated Tga20, Tga20xKO and
622 Tga20xN158D mouse brains. 10% brain homogenates from 22L, ME7, 301C and RML
623 inoculated Tga20, Tga20xKO and Tga20xN158D mice were digested with 80 µg/ml of Protease-
624 K (PK). Digested samples were analyzed by Western blot using SAF83 (1:400). No significant
625 differences are observed between any of the Tga20, Tga20xKO and Tga20xN158D brain
626 homogenates suggesting that N158D PrP^{C} did not alter the major biochemical characteristics
627 of any of the four prion strains. Control: Undigested Tga20xKO brain homogenate. Mw:
628 Molecular weight.

629

630 **Fig. S1** PrP expression levels from Tga20, Tga20xN158D, Tga20xKO and TgN158D mouse brains.
631 10% brain homogenates from Tga20, Tga20xN158D, Tga20xKO and TgN158D mice were
632 diluted 1:40, 1:80, 1:160, 1:320, 1:640 and 1:1280 and were analyzed by Western blot using
633 monoclonal antibodies 5C6 (1:2,000) which does not bind N158D PrP, and SAF83 (1:400) able
634 to bind both types of proteins. The N158D PrP from Tga20xN158D and TgN158D mice is not
635 observed when 5C6 monoclonal antibody is used but the use of SAF83 shows how the PrP
636 expression levels of Tga20, Tga20xN158D, Tga20xKO and TgN158D are approximately ~8x,
637 ~4x+~2x, ~4x+0x and ~4x compared to wt mouse PrP^{C}, respectively based on signal intensity.
638 No significant differences are observed in the electrophoretic migration patterns. Mw:
639 Molecular weight.

640

641 **Fig. S2** Histological localization of PrP^C in Tga20xTgN158D and TgN158D mouse brains. **(a)**
642 Immunohistochemical detection of PrP^C in neurons of the deep cerebellar nuclei from a
643 Tga20xN158D and a TgN158D mouse using 5C6 and SAF32 monoclonal antibodies. 5C6
644 antibody produces intense immunostaining in the Tga20xN158D mouse brain, corresponding
645 to a mouse wt PrP staining, since this antibody does not recognize N158D PrP. Accordingly, no
646 immunostaining is observed in the TgN158D mouse using the same antibody. However, SAF32
647 produces a strong immunolabeling in a serial histological section from the same animal
648 showing the distribution of N158D PrP. Similar immunolabeling is observed between
649 Tga20xN158D and TgN158D mice using SAF32 antibody. **(b)** TgN158D mouse brain serial
650 optical z-sections by confocal microscopy (x40). To more clearly determine the localization of
651 N158D PrP, fluorescence emission from a TgN158D mouse brain, stained using SAF32
652 antibody, was analyzed using confocal microscopy. The fluorescence emission resulted from
653 excitation with 594-nm laser and was detected using long-pass 615-nm filter. 0,5 µm z-stacks
654 of digital images were captured using Zen 2008 software (Carl Zeiss Microimaging) with 40x
655 (NA 1.3) objective. A very intense neuronal staining of N158D PrP is observed. N158D PrP was
656 detected in the neuronal membrane (arrows).

657

658 **Fig. S3** PrP^{res} detection from 22L inoculated Tga20xKO and Tga20xN158D mouse brains using a
659 monoclonal antibody unable to bind N158D PrP. 10% brain homogenates from 22L inoculated
660 Tga20xKO and Tga20xN158D mice were digested with 80 µg/ml of Protease-K (PK) and then
661 diluted 1:2, 1:4, 1:8, 1:16, 1:32 and 1:64. Digested samples were analyzed by Western blot
662 using two monoclonal antibodies subsequently: first, 5C6 (1:2,000) which does not bind N158D
663 PrP, and later, using the same membrane, SAF83 (1:400) able to bind both types of proteins.
664 No significant differences are observed between both blots indicating that N158D PrP was not

converted at least at the level to be distinguished by this technique. Control: Undigested Tga20xKO brain homogenate. Mw: Molecular weight.

Fig. S4 PrP^{res} detection from RML inoculated Tga20xKO and Tga20xN158D mouse brains. 10% brain homogenates from RML inoculated Tga20xKO and Tga20xN158D mice, selected with different days post inoculation (dpi) were digested with 80 µg/ml of Protease-K (PK). Digested samples were analyzed by Western blot using SAF83 (1:400) and the signal level of PrP^{res} are compared. Despite the RML inoculated Tga20xKO mice were culled at ~90 dpi, the amounts of PrP^{res} are significant higher than the observed in the RML inoculated Tga20xN158D mice. This result suggests that the elongation of the incubation times in this model is likely due to a slower conversion of the wt PrP^{C}. Control: Undigested Tga20xKO brain homogenate. Mw: Molecular weight.

Figure 1

Click here to download Figure Fig1x2.pdf

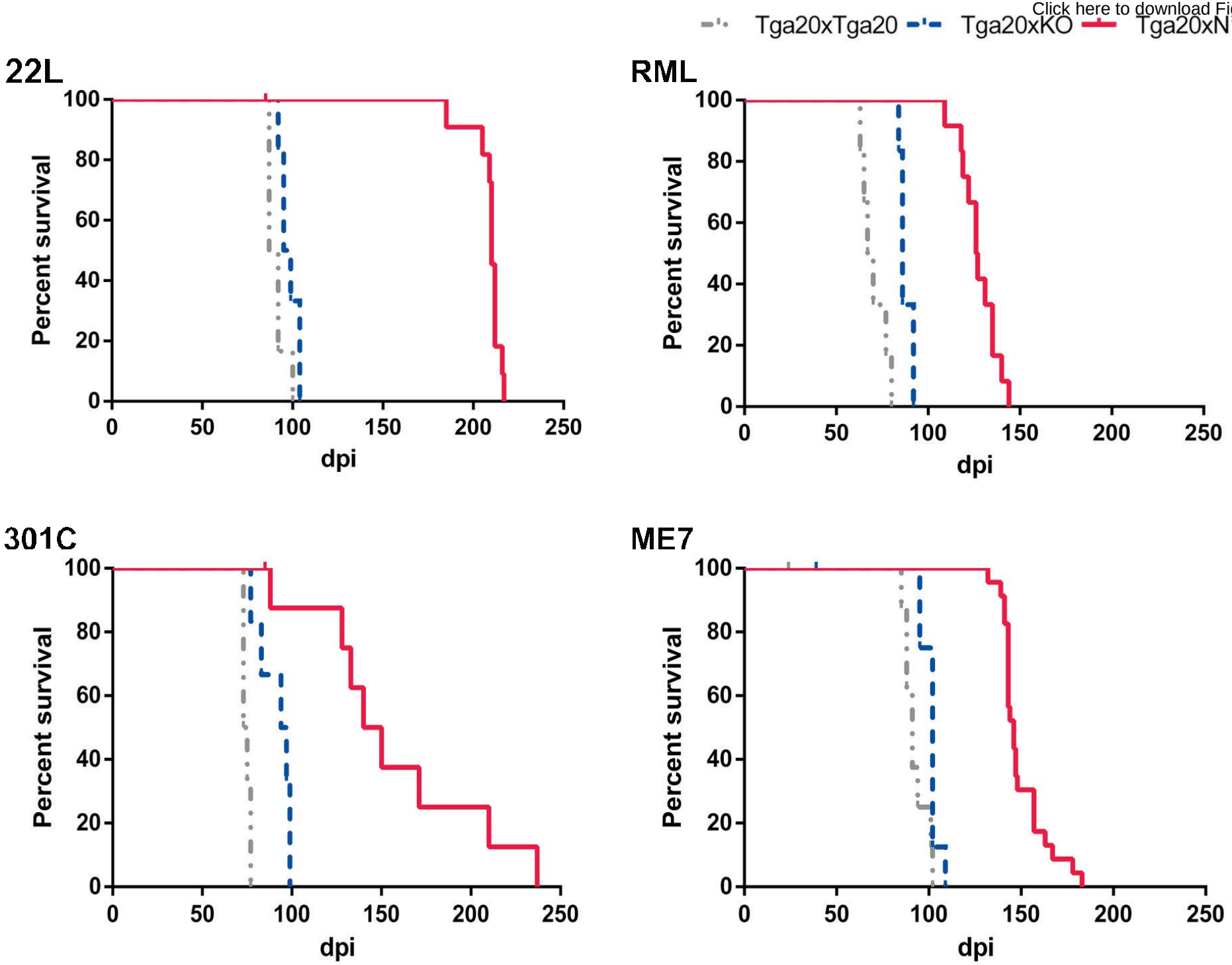

Figure 2

Click here to download Figure Fig2x2.pdf

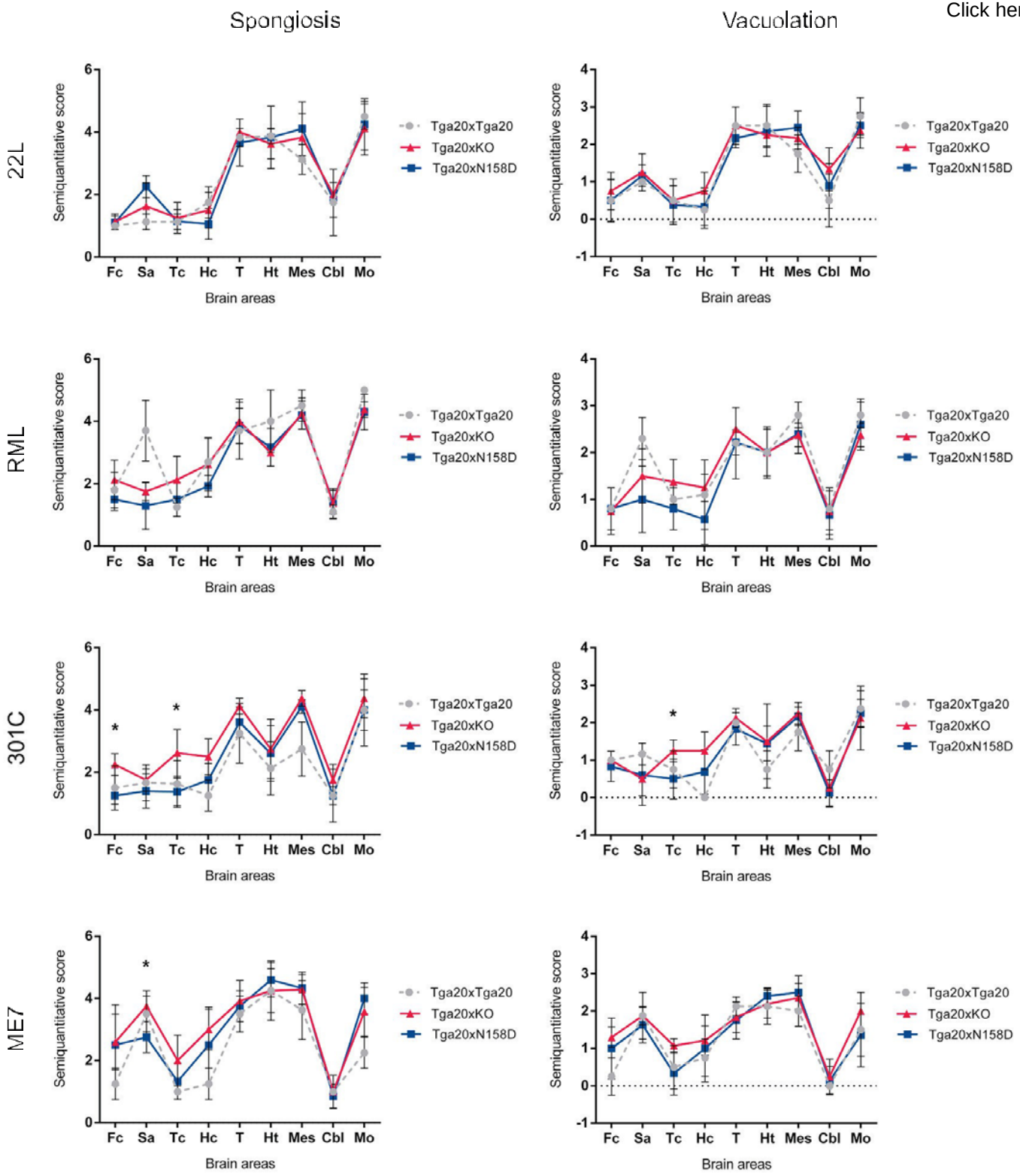

Figure 3

Click here to download Figure Fig3x2.pdf

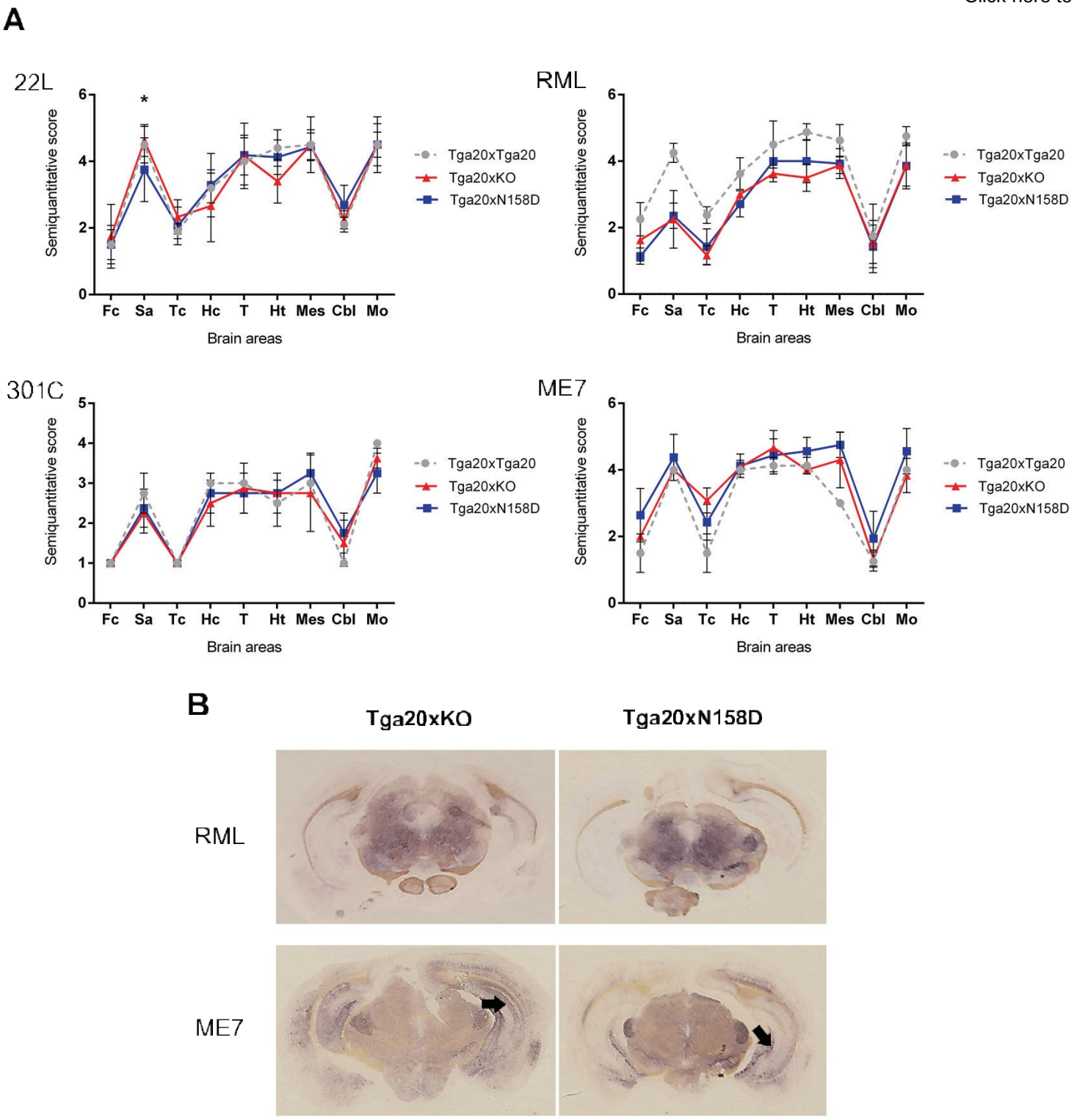

Figure 4

Click here to download Figure Fig4.tif

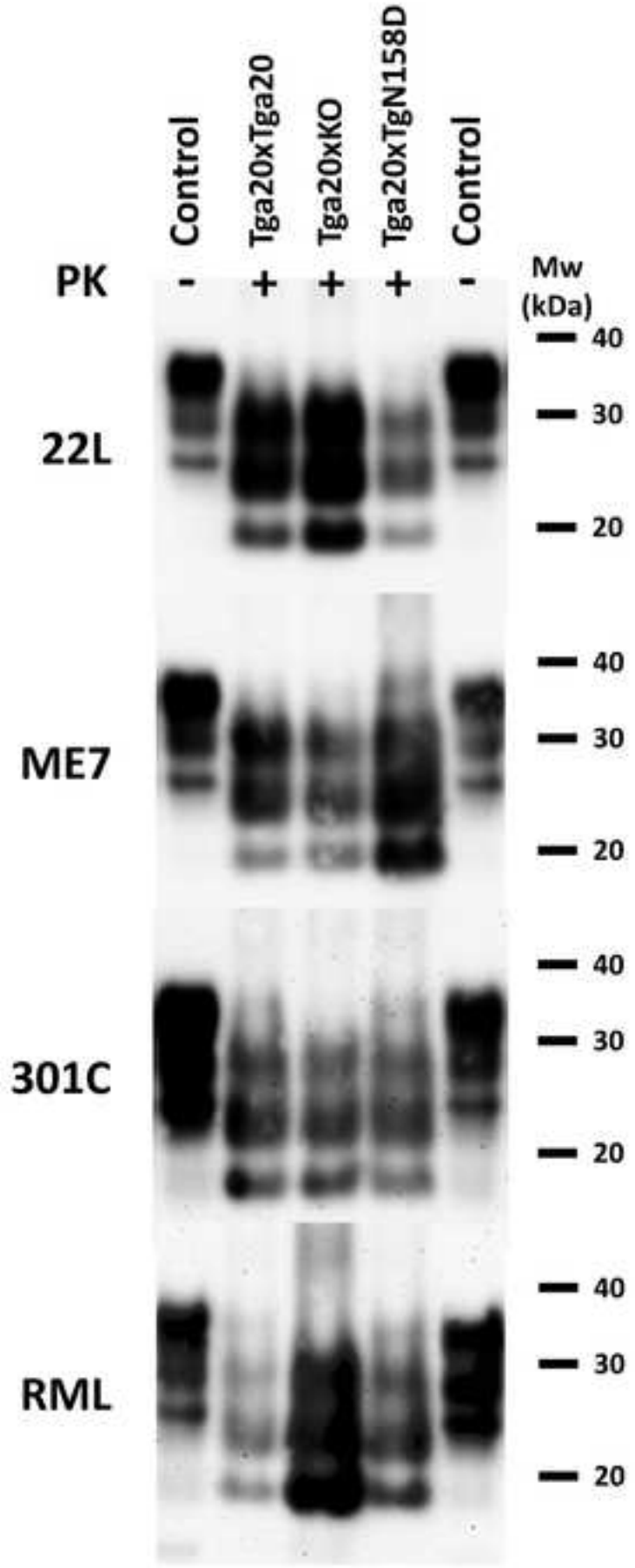

Supplementary Material

An amino acid substitution found in animals with low susceptibility to prion diseases confers a protective dominant-negative effect in prion-infected transgenic mice

Alicia Otero [1], Rosa Bolea [1], Carlos Hedman [1], Natalia Fernández-Borges [2], Belén Marín [1], Óscar López-Pérez [1, 3], Tomás Barrio [1], Hasier Eraña [2], Manuel A. Sánchez-Martín [4,5], Marta Monzón [1], Juan José Badiola [1], Joaquín Castilla [2, 6]*

[1] Centro de Encefalopatías y Enfermedades Transmisibles Emergentes, Facultad de Veterinaria, Universidad de Zaragoza, Zaragoza, Spain.

[2] CIC bioGUNE, Parque Tecnológico de Bizkaia, Derio, Bizkaia, Spain.

[3] Laboratorio de Genética Bioquímica (LAGENBIO), Facultad de Veterinaria, Universidad de Zaragoza, Zaragoza, Spain.

[4] Servicio de Transgénesis, Nucleus, Universidad de Salamanca, Salamanca, Spain.

[5] IBSAL, Instituto de Investigación Biomédica de Salamanca, Salamanca, Spain.

[6] IKERBASQUE, Basque Foundation for Science, Bilbao, Bizkaia, Spain.

*** Corresponding author:**

Joaquín Castilla

CIC bioGUNE

Parque tecnológico de Bizkaia

Derio 48160, Bizkaia, Spain

E-mail: castilla@joaquincastilla.com

Fig. S1 PrP expression levels from Tga20, Tga20xN158D, Tga20xKO and TgN158D mouse brains. 10% brain homogenates from Tga20, Tga20xN158D, Tga20xKO and TgN158D mice were diluted 1:40, 1:80, 1:160, 1:320, 1:640 and 1:1280 and were analyzed by Western blot using monoclonal antibodies 5C6 (1:2,000) which does not bind N158D PrP, and Saf83 (1:400) able to bind both types of proteins. The N158D PrP from Tga20xN158D and TgN158DxTgN158D mice is not observed when 5C6 monoclonal antibody is used but the use of Saf83 shows how the PrP expression levels of Tga20, Tga20xN158D, Tga20xKO and TgN158D are approximately ~8x, ~4x+~2x, ~4x+0x and ~4x compared to wild-type mouse PrP^{C}, respectively based on signal intensity. No significant differences are observed in the electrophoretic migration patterns. Mw: Molecular weight.

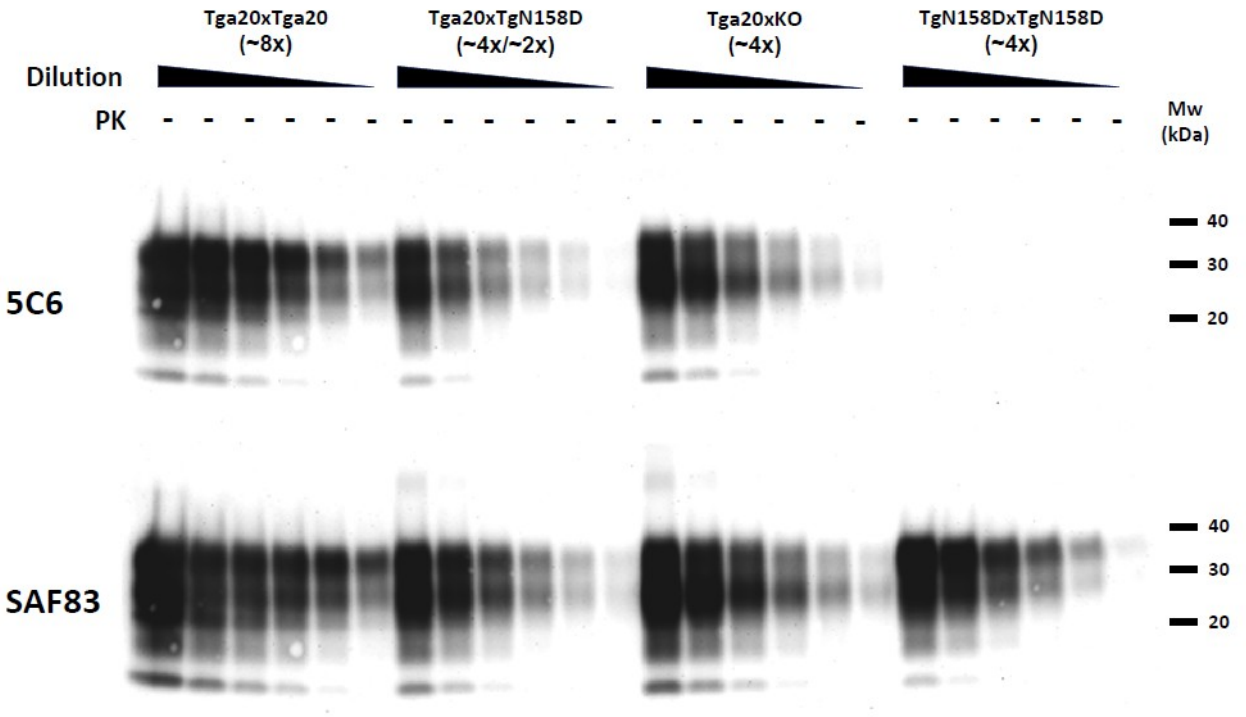

Fig. S2 Histological localization of PrP^C in Tga20xTgN158D and TgN158D mouse brains. **(a)** Immunohistochemical detection of PrP^C in neurons of the deep cerebellar nuclei from a Tga20xN158D and a TgN158D mouse using 5C6 and Saf32 monoclonal antibodies. 5C6 antibody produces intense immunostaining in the Tga20xN158D mouse brain, corresponding to a mouse wildr-type PrP staining, since this antibody does not recognize N158D PrP. Accordingly, no immunostaining is observed in the TgN158D mouse using the same antibody. However, Saf32 produces a strong immunolabeling in a serial histological section from the same animal showing the distribution of N158D PrP. Similar immunolabeling is observed between Tga20xN158D and TgN158D mice using Saf32 antibody. **(b)** TgN158D mouse brain serial optical z-sections by confocal microscopy. To more clearly determine the localization of N158D PrP, fluorescence emission from a TgN158DxTgN158S mouse brain, stained using Saf32 antibody, was analyzed using confocal microscopy. Serial 0.5 µm z-sections of medulla oblongata from this mouse were obtained using a green helium/neon (543 nm) laser system. A very intense neuronal staining of N158D PrP is observed. N158D PrP was detected in the neuronal membrane (arrows).

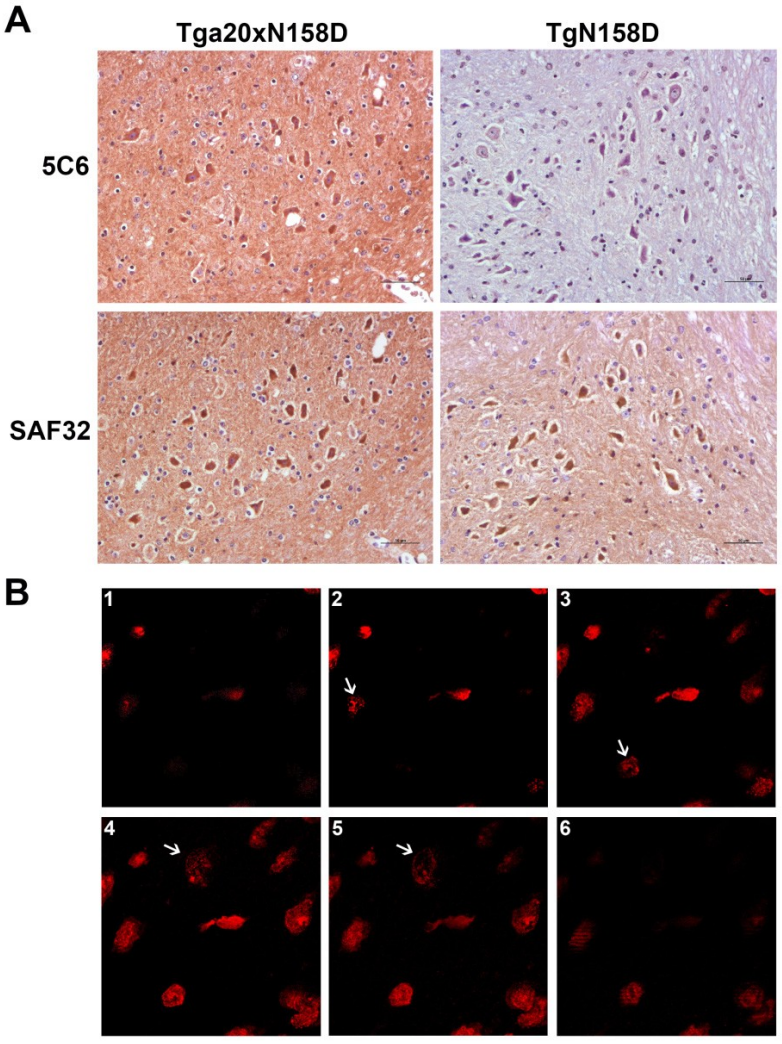

Fig. S3 PrP^{res} detection from 22L inoculated Tga20xKO and Tga20xN158D mouse brains using a monoclonal antibody unable to bind N158D PrP. 10% brain homogenates from 22L inoculated Tga20xKO and Tga20xN158D mice were digested with 80 µg/ml of Protease-K (PK) and then diluted 1:2, 1:4, 1:8, 1:16, 1:32 and 1:64. Digested samples were analyzed by Western blot using two monoclonal antibodies subsequently: first, 5C6 (1:2,000) which does not bind N158D PrP, and later, using the same membrane, Saf83 (1:400) able to bind both types of proteins. No significant differences are observed between both blots indicating that N158D PrP was not converted at least at the level to be distinguished by this technique. Control: Undigested Tga20xKO brain homogenate. Mw: Molecular weight.

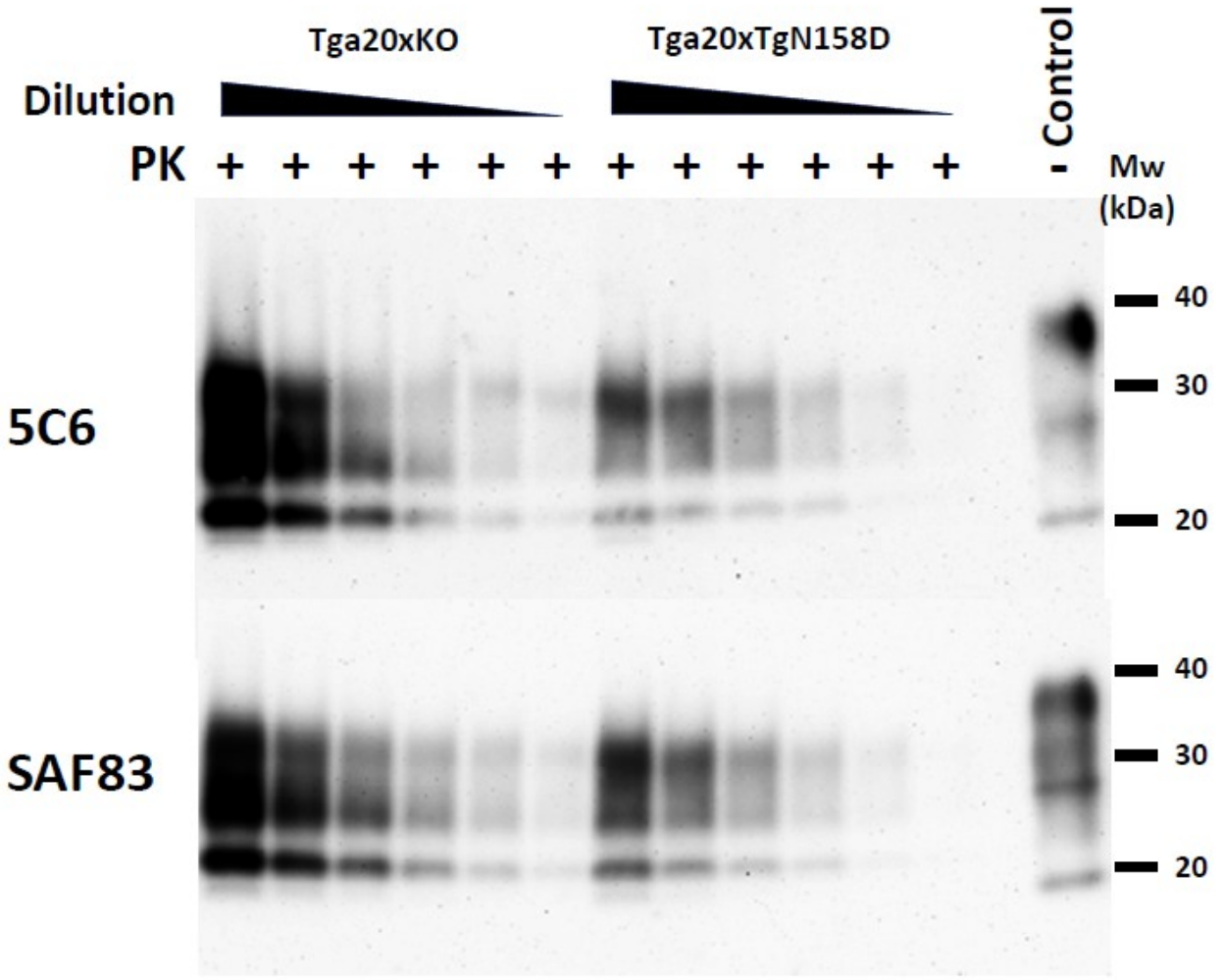

Fig. S4 PrP^{res} detection from RML inoculated Tga20xKO and Tga20xN158D mouse brains. 10% brain homogenates from RML inoculated Tga20xKO and Tga20xN158D mice, selected with different days post inoculation (dpi) were digested with 80 µg/ml of Protease-K (PK). Digested samples were analyzed by Western blot using Saf83 (1:400) and the signal level of PrP^{res} are compared. Despite the RML inoculated Tga20xKO mice were culled at ~90 dpi, the amounts of PrP^{res} are significant higher than the observed in the RML inoculated Tga20xN158D mice. This result suggests that the elongation of the incubation times in this model is likely due to a slower conversion of the wild-type PrP^{C}. Control: Undigested Tga20xKO brain homogenate. Mw: Molecular weight.